Bibliographical reference

Guideline for Adopting the Local Reaction Assumption for Porous Absorbers in Terms of Random Incidence Absorption Coefficients, Cheol-Ho Jeong, Acta Acustica **vol. 97** (Number 5), 2011, pp. 779-790

DOI

https://doi.org/10.3813/AAA.918458

Acta Acustica united with Acustica
Vol. 97 (2011) 779 – 790

DOI 10.3813/AAA.918458

Guideline for Adopting the Local Reaction Assumption for Porous Absorbers in Terms of Random Incidence Absorption Coefficients

Cheol-Ho Jeong
Acoustic Technology, Department of Electrical Engineering, Technical University of Denmark, 2800, Kongens Lyngby, Denmark. chj@elektro.dtu.dk

Summary
Room surfaces have been extensively modeled as locally reacting in room acoustic predictions although such modeling could yield significant errors under certain conditions. Therefore, this study aims to propose a guideline for adopting the local reaction assumption by comparing predicted random incidence acoustical characteristics of typical building elements made of porous materials assuming extended and local reaction. For each surface reaction, five well-established wave propagation models, the Delany-Bazley, Miki, Beranek, Allard-Champoux, and Biot model, are employed. Effects of the flow resistivity and the absorber thickness on the difference between the two surface reaction models are examined and discussed. For a porous absorber backed by a rigid surface, the assumption of local reaction always underestimates the random incidence absorption coefficient and the local reaction models give errors of less than 10% if the thickness exceeds 120 mm for a flow resistivity of 5000 $\mathrm{Nm^{-4}s}$. As the flow resistivity doubles, a decrease in the required thickness by 25 mm is observed to achieve the same amount of error. For an absorber backed by an air gap, the thickness ratio between the material and air cavity is important, since the thicker the cavity, the more extendedly reacting the absorber. If the absorber thickness is approximately 40% of the cavity depth, the local reaction models give errors below 10% even for a low flow resistivity case.
PACS no. 43.55.Ev

1. Introduction

Modeling surfaces in room acoustic predictions is not a straightforward process. Relevant acoustic properties are surface impedances, pressure reflection coefficients, and sound absorption coefficients, which are all dependent on frequency and angle of incidence. In practice, some simplifications can be made. As a crude simplification, many geometrical acoustics methods have assumed that the absorption coefficients of room surfaces are independent of incidence angle and constant over a frequency octave band. Another well-known simplification is local reaction, implying that the surface impedance does not change with angle of incidence. However, extended reaction is considered physically more correct, in particular for porous media backed by an air space, etc. A number of wave propagation models in absorbing materials are available for predicting the absorption characteristics, to name a few, an empirical model by Delany and Bazley [1], a modification of Delany and Bazley's model by Miki [2], a theoretical model by Beranek [3], a phenomenological and rigid frame model by Allard and Champoux [4] and a poroelastic frame model by Biot [5].

Received 24 February 2011,
accepted 15 May 2011.

The major applications of sound absorbing surfaces include duct acoustics, outdoor sound propagation, and room acoustics. In duct acoustics, many attempts with extended reaction models have been undertaken in order to identify the effects of extended reaction of the lining materials in dissipative silencers [6]. For example, Kurze and Vér ascribed the shift of the attenuation peaks to an increased stiffness of the extendedly reacting lining materials at oblique angles [7]. Many studies have been carried out in outdoor sound propagation, which also mainly deals with near grazing incidence cases in semi-free spaces (for example, [8]). A similar result is expected for porous materials used in rooms; however, it is noted that the main difference between applications in room acoustics and those in other areas of acoustics is the incident direction of waves: The main direction of incidence in dissipative silencers is grazing incidence, whereas the incidence angles of waves in rooms are rather uniformly distributed. To the author's knowledge, only a very limited number of such studies have been performed in room acoustics. To name a few studies that have modeled boundary surfaces as bulk reacting, one could mention a boundary element model by Utsuno *et al.* [9], an angle by angle approach by Franzoni and Elliott [10], and a beam tracing study by Hodgson and

Wareing [11]. They all concluded that modeling surfaces as of extended reaction agrees better with measurements.

In room acoustics, frequency averaged random incidence absorption coefficients in 1/1 or 1/3 octave bands are the most frequently used quantities, for example, absorption coefficients as input data in geometrical acoustics simulations, in theoretical predictions such as the Sabine formula, and in noise level estimation. Therefore, the main parameter of the present study is the random incidence absorption coefficient averaged in octave bands. Angularly varying absorption coefficients and surface impedances, however, are also investigated to account for discrepancies between the two reaction models. Two typical building elements are studied: porous materials backed by a rigid wall and porous materials backed by an air cavity.

There are two crucial questions behind this study: The first question is, "In which conditions the two surface reaction models yield similar random incidence absorption coefficients?", since many authors have assumed locally reacting surfaces without clarifying the limitations of such an assumption. It is often said that as the flow resistivity increases, surfaces can be modeled as of local reaction, but it is difficult to find any quantitative guideline in the literature. The thickness of an absorber and the thickness ratio of an absorber to an air cavity are also decisive factors determining the difference between the two surface reaction models. This study primarily aims to propose a useful guideline for adopting local reaction assumption for porous materials for the two mounting conditions.

The second question is, "should one use the Biot model, although it requires many parameters in predicting absorption coefficients?". The Biot model is well established and is regarded as the most accurate model with experimental validations [12, 13], but it is far more complicated than the other models, making it the least practical one. Therefore the second aim is to investigate the variations in the random incidence absorption coefficient predicted by the wave propagation models.

2. Surface reaction models

2.1. Local reaction

The simplest surface reaction model assumes that the wave transmitted into a porous material is refracted so that it propagates effectively only perpendicular to the surface [14]. This is referred to as a normally reacting, locally reacting, or point reacting surface. This is likely to happen in anisotropic solids such as honeycomb structures, where the waves are forced to propagate perpendicular to the surface. Local reaction is also related to the ratio of the incident wave speed to the transmitted wave speed. Local reaction occurs, when the speed of the compressional wave in air is much higher than that of waves in an anisotropic solid, $c_t \ll c_i$, where the subscripts i and t denote the incidence and transmitted, respectively. By Snell's law, the angle of transmission, θ_t, becomes much less than the incidence angle, θ_i, resulting in a marked bending of the transmitted wave towards the normal direction. Therefore, it is reasonable to assume that the ratio of acoustic pressure acting on the surface to the normal fluid velocity is independent of the incidence angle. Once the surface impedance of an infinite panel for normal incidence of a plane wave is known, the absorption characteristic of the surface is readily obtained,

$$\alpha^l(f,\theta_i) = 1 - \left| \frac{Z(f,0) - \rho_0 c_0/\cos\theta_i}{Z(f,0) + \rho_0 c_0/\cos\theta_i} \right|^2. \qquad (1)$$

Here, $Z(f,0)$ is the surface impedance of the material at normal incidence, ρ_0 the air density, and c_0 the speed of sound in lossless air. Note that the reflection/absorption coefficient varies with the incidence angle, although the surface impedance is constant for all directions of incidence.

The assumption of local reaction has been widely used in room acoustic simulations, both using wave based methods and geometrical acoustics. The main reason is its simplicity compared with non-local reaction models, since knowledge of the normal surface impedance suffices for calculating the absorption characteristic of the wall, whereas the extended reaction models as a minimum necessitate a characteristic impedance and propagation constant. However, the adequacy of the assumption of local reaction is questionable for porous layers backed by an air cavity, since the refracted wave in the air cavity will propagate in the same direction as the initial incidence angle according to Snell's law.

2.2. Extended reaction

Extended reaction is also referred to as bulk reaction or non-local reaction. The angle of transmission is determined by Snell's law, and waves are no longer transmitted in the perpendicular direction to the surface of interest. Many authors have measured significant extended reaction in porous materials, for instance [15, 16, 17, 18]. Of the various theories on extended reaction characteristics, a homogeneous (material properties are spatially uniform) and isotropic (material properties are independent of directions) porous material is assumed in what follows, although it is not always valid, because the orientation of the fibers in the manufacturing process, the variation in the fiber size, and the distribution of bonding agent may cause the material to become anisotropic. If the porous material of interest is regarded as an equivalent homogeneous fluid medium, propagation of sound can be characterized by the characteristic impedance, Z_c, and the propagation constant, γ ($= \mathrm{j}k_t = \mathrm{j}\omega/c_t$), where k_t is the complex wave number in the equivalent fluid medium. For a material having a thickness d and backed by another material with a surface impedance of $Z|_{x=d}$, the surface impedance in front of the entire construction at $x = 0$ for a plane wave incident at an angle θ_i is [12]

$$Z(f,\theta_i) = \frac{Z_c k_0}{k_x}\left[\frac{-\mathrm{j}Z|_{x=d}\cot(k_x d) + Z_c\, k_0/k_x}{Z|_{x=d} - \mathrm{j}Z_c\,(k_0/k_x)\cot(k_x d)}\right], \qquad (2)$$

where k_0 is the wave number in air, k_x is the normal component of k_t ($= \sqrt{k_t^2 - k_0^2 \sin^2\theta_i}$), and j is the imaginary

unit. Note that $k_y = k_t \sin(\theta_t) = k_0 \sin(\theta_i)$ by Snell's law. If the backing surface is acoustically rigid ($Z|_{x=d} = \infty$), equation (2) becomes $Z(f,\theta) = -\mathrm{j}Z_c(k/k_x)\cot(k_x d)$. For absorbers backed by an air cavity, $Z|_{x=d}(f,\theta_i)$ can be substituted by $-\mathrm{j}(\rho_0 c_0 k_0/k_x)\cot(k_0 d_0 \cos\theta_i)$, where d_0 is the cavity depth. From the surface impedance in equation (2), the absorption coefficient becomes

$$\alpha^e(f,\theta_i) = 1 - \left| \frac{Z(f,\theta_i) - \rho_0 c_0/\cos\theta_i}{Z(f,\theta_i) + \rho_0 c_0/\cos\theta_i} \right|^2 . \qquad (3)$$

Note that the normal incidence surface impedance $Z(f,0)$ in equation (1) for the local-reaction absorption coefficient is obtained by setting θ_i to zero in equation (2).

There are two approaches to obtain the characteristic impedance and the propagation constant: an empirical and an analytical approach [13]. The Delany and Bazley model is the most widely used empirical model, based on a regression model with only one variable, the frequency divided by the specific flow resistance [1]. Modified versions of the Delany and Bazley model, the Miki [2], Mechel [19], and Komatsu model [20], may also be categorized as empirical models.

On the other hand, the Beranek model is a fully analytical model, based on the wave equation under assumption of an isothermal process. Analytical wave propagation models are classified in two groups: rigid-frame [4] and elastic frame models [5]. In the former, a single compressional wave propagates under either perfectly rigid or perfectly limp conditions. The propagation is governed by the Helmholtz equation, in which the equivalent fluid is characterized by two parameters, an effective density and an effective bulk modulus, accounting for the viscous and thermal dissipation of the acoustic wave. The rigid frame implies that no deformation is undergone under acoustic excitation. On the contrary, when the frame does not resist external excitations and its stress field vanishes, the frame is assumed to be limp. This happens, e.g., if solid particles are suspended in a fluid medium or if the in-vacuo stiffness of the solid phase is far less than that of the fluid phase. For porous materials with an elastic solid frame (called poroelastic materials), the Biot model is the best known theory, which supports two compressional waves and one shear wave for fluid saturated poroelastic media, particularly emphasizing the elasticity of the solid frame [5]. The solid motion is described by the frame density, the frame shear modulus (generally a complex quantity), the Poisson ratio of the frame. The Biot theory requires a number of parameters, most of which are not well known for building surfaces. Therefore its practical applicability is quite limited. The other four models are regarded as equivalent fluid models, since the porous material is modelled as an equivalent fluid, where only the air borne wave can propagate in the air pores.

The wave propagation models require several parameters in order to explain the behavior of sound in a mixed structure of fluid and solid frame. The primary parameter is the flow resistivity. A second important parameter might be the porosity, ϵ, the ratio of the total pore volume to the total volume of the absorber. Good absorbers tend to have a porosity approaching unity, and often assumed to lie between 0.95 and 1 [13]. These two parameters are relatively easily measured in laboratories.

There are secondary parameters, such as the tortuosity (k_s), the characteristic dimensions (Λ and Λ', which are referred to as the viscous characteristic length and the thermal characteristic length, respectively), and so on. The tortuosity is the degree of complexity of the propagation paths that cause efficient attenuation of sound in air-saturated porous media. In the simplest case of cylindrical pores all aligned in the same direction, the tortuosity is related to the angle between the pores and the incident sound direction. However, actual porous absorbers are not manufactured in a well-ordered way, and the tortuosity should be obtained experimentally. The characteristic dimensions are more complicatedly defined: the characteristic dimension is a weighted ratio of the volume to surface area of the pores, and the second characteristic dimension is given by the ratio of the volume to the surface area of the pores, multiplied by 2 [12, 13]. References [12, 13] are recommended for more information on these parameters. Since these parameters are rarely reported for building materials, the Biot and Allard-Champoux model are barely applied in practice. Note that the Biot model additionally necessitate the frame density, the frame shear modulus (generally a complex quantity), the Poisson ratio of the frame.

The two surface reaction models should give the same results at nearly normal incidence. As the angle of incidence increases, the differences tend to become noticeable. Nevertheless, in duct acoustics, some investigations have demonstrated that lined ducts under assumption of local reaction agree well with experiments at low frequencies, in particular for a thin lining material [21, 22, 23]. This conclusion is contradictory to the common expectation that the two surface reaction models differ noticeably for oblique incidences. It has been reported that the difference between the two models becomes significant with increasing frequency, whereas Hodgson and Wareing showed contradictory results [11]. Possible explanations to such contradictions will be discussed in sections 3 and 4.

A brief introduction to the five wave propagation models follows. Wave motion in an equivalent fluid medium can be modeled with two complex quantities, the propagation constant and the characteristic impedance, or with the effective density and the bulk modulus.

2.2.1. Delany and Bazley's empirical power law (DB model)

The best known empirical model was suggested by Delany and Bazley [1]. They measured characteristic impedances and propagation constants of fibrous absorbent materials and established power law relationships with the frequency divided by flow resistivity (in $\mathrm{Nm^{-4}s}$), f/σ, by regression analyses. They measured approximately 200 data points in the frequency range from 250 Hz to 4000 Hz, and the flow resistance ranged from 2000 to 80000 MKS Rayls. The power law functions are applicable within a

range of $0.01 < f/\sigma < 1$ (in SI units).

$$Z_c = \rho_0 c_0 \left(1 + 0.0495\left(\frac{f}{\sigma}\right)^{-0.754} - \mathrm{j}0.0754\left(\frac{f}{\sigma}\right)^{-0.732}\right), \tag{4a}$$

$$k = \frac{\omega}{c_0}\left(1 + 0.0848\left(\frac{f}{\sigma}\right)^{-0.700} - \mathrm{j}0.164\left(\frac{f}{\sigma}\right)^{-0.595}\right). \tag{4b}$$

In room acoustics, absorption coefficients are usually required in 1/3 or 1/1 octave bands, from 63 (or 125) Hz to 4000 (or 8000) Hz. Considering the fact that the typical range of the flow resistivity varies from 4000 $\mathrm{Nm^{-4}s}$ to 50000 $\mathrm{Nm^{-4}s}$ and extrapolation of the model is strongly avoided [1, 2], this empirical model cannot be used at frequencies below 0.01σ.

2.2.2. Miki's modification (MK model)

Since the DB model gives erroneous prediction when $f < 0.01\sigma$ [2, 4], Miki developed a different regression model by taking causality into account using the same empirical dataset as Delany and Bazley [2],

$$Z_c = \rho_0 c_0 \left(1 + 0.070\left(\frac{f}{\sigma}\right)^{-0.632} - \mathrm{j}0.107\left(\frac{f}{\sigma}\right)^{-0.632}\right), \tag{5a}$$

$$k = \frac{\omega}{c_0}\left(1 + 0.109\left(\frac{f}{\sigma}\right)^{-0.618} - \mathrm{j}0.160\left(\frac{f}{\sigma}\right)^{-0.618}\right). \tag{5b}$$

2.2.3. Beranek's model (BR model)

Beranek assumed that gaseous expansions are isothermal in most of the audio-frequency range in materials made of finely divided particles. Under such an assumption, the speed of sound, c_1, is equal to $c_0/1.18$, and the effective density, ρ_1, is assumed to be the same as ρ_0 [3]. He argued that the assumption is true at least at frequencies below 2000 Hz on the basis of his experimental validation, but the upper limit frequency cannot be determined by investigating a few absorbers. The three main parameters are the flow resistivity, σ, the porosity ε, and the effective density of the gas particle, ρ_1. According to [3], the surface impedance for a rigidly backed material of a thickness d is given by

$$Z(f,\theta_i) = \rho_1 c_1 \frac{\sqrt{1 - \mathrm{j}\frac{\sigma}{\rho_1\omega}}}{\sqrt{\varepsilon}\sqrt{1 - \frac{c_2^2}{c_0^2}\sin^2\theta_i}} \cdot \coth\left(\mathrm{i}\frac{\omega d}{c_2}\sqrt{1 - \frac{c_2^2}{c_0^2}\sin^2\theta_i}\right), \tag{6}$$

where $c_2 = c_1/\sqrt{\varepsilon(1 - \mathrm{j}\sigma/(\rho_1\omega))}$ and the surface impedance for a material in front of an air backing depth of d_0 is given by

$$Z(f,\theta_i) = \rho_1 c_1 \frac{\sqrt{1 - \mathrm{j}\frac{\sigma}{\rho_1\omega}}}{\sqrt{\varepsilon}\sqrt{1 - \frac{c_2^2}{c_0^2}\sin^2\theta_i}} \cdot \coth\left(\mathrm{i}\frac{\omega\sqrt{\varepsilon}d}{c_2}\sqrt{1 - \mathrm{j}\frac{\sigma}{\rho_1\omega}}\sqrt{1 - \frac{c_2^2}{c_0^2}\sin^2\theta_i} + \psi\right), \tag{7}$$

where

$$\psi = \coth^{-1}\left(\frac{\rho_0 c_0}{\rho_1 c_1}\frac{\sqrt{1 - \frac{c_2^2}{c_0^2}\sin^2\theta_i}}{\sqrt{1 - \mathrm{j}\frac{\sigma}{\rho_1\omega}}}\frac{(-\mathrm{j})\sqrt{\varepsilon}\cot\left(\frac{\omega}{c_0}d_0\cos\theta_i\right)}{\cos\theta_i}\right).$$

Here, c_1 is the speed of sound under isothermal condition and c_2 is named as the phase speed of propagation in the porous material. Note, however, that c_2 may not be correct, since the phase speed in the porous medium is likely to be derived to $c_1/\sqrt{1 - \mathrm{j}\sigma\varepsilon/(\rho_1\omega)}$. In this study, c_2 in equation (6) was used in calculating the acoustical quantities by the BR model.

2.2.4. A phenomenological model (AC model)

A semi-analytic phenomenological, rigid frame model by Allard and Champoux [4, 24] based on Johnson's investigation [25] is included in the present study. On the assumption of a rigid frame, the effective density of the porous material and the dynamic bulk modulus are given by [13]:

$$\rho_e = k_s\rho_0\left(1 + \frac{\sigma\varepsilon}{\mathrm{j}\omega\rho_0 k_s}\sqrt{1 + \frac{4\mathrm{j}k_s^2\eta\rho_0\omega}{\sigma^2\Lambda^2\varepsilon^2}}\right), \tag{8a}$$

$$K_e = \frac{\gamma P_0}{\gamma - (\gamma-1)\left(1 + \frac{8\eta}{\mathrm{j}\Lambda'^2 N_p\omega\rho_0}\sqrt{1 + \frac{\mathrm{j}\rho_0 N_p\omega\Lambda'^2}{16\eta}}\right)^{-1}}, \tag{8b}$$

where k_s is the tortuosity, η is the viscosity of air ($18.6 \cdot 10^{-6}$ Pa s), N_p is the Prandtl number (=0.72), γ is the specific heat ratio (=1.4), P_0 is the atmospheric pressure (=101.32 kPa), and ω is the angular frequency. From the effective density and bulk modulus, the characteristic impedance and the propagation wavenumber are found by

$$Z_c = \sqrt{\rho_e K_e}, \qquad k = \omega\sqrt{\frac{\rho_e}{K_e}}. \tag{9}$$

The frequency dependent dynamic density was proposed in order to take account of the inertial and viscous coupling between the air and the rigid frame. At high frequencies, the dynamic density approaches to $k_s\rho_0$. In terms of the bulk modulus, the value converges to P_0 and γP_0 at low and high frequencies, representing low frequency isothermal and high frequency adiabatic behavior.

Table I. Required parameters for calculating absorption coefficients. *DB* is an acronym for the Delany and Bazley model, *MK* for the Miki model, *BR* for the Beranek model, *BT* for the Biot model. σ: Flow resistivity [Nm^{-4}s], ε: Porosity, c_1: Isothermal effective speed, k_s: Tortuosity, (Λ, Λ'): Characteristic dimensions. Fd/Fs/Pr is an abbreviation for Frame density / Frame shear modulus / Poisson ratio.

	DB and *MK*	*BR*	*AC*	*BT*
σ	X	X	X	X
ε		X	X	X
c_1		X		
k_s			X	X
(Λ, Λ')			X	X
Fd/Fs/Pr				X

2.2.5. Biot's model based on an elastic solid frame (BT model)

This model supports two compressional waves and one shear wave for air-saturated poroelastic media. For a weak coupling between the frame and air, the air-borne compressional wave propagates mostly through the pores, whereas the frame-borne compressional wave can propagate in both the frame and air. The third wave is the frame-borne shear wave, which is barely affected by air and very similar to an in-vacuo shear wave of the frame.

The resonance of the frame-borne wave sometimes can be observed in measured surface impedance data, which can be accounted for only by the Biot model. A peak appears in the imaginary part of the impedance around the $\lambda/4$ resonance at the normal incidence [12].

A transfer matrix approach for multiple layers, which is well described in [11, 12], is employed in the present study. By combining the transfer matrices of a isotropic poroelastic layer and a fluid layer (only if the poroelastic layer is backed by an air gap) and the interface matrices for matching the boundary conditions of adjacent layers into a system transfer matrix, one can obtain the acoustical properties such as the surface impedance for all frequencies and angles of incidence. Table I lists required parameters for the five wave propagation models. The Biot model requires a lot of parameters, whereas the Delany-Bazley and Miki model require the least information, which is the flow resistivity.

3. Random incidence absorption coefficient

Two building elements made of porous materials have been studied: porous layers backed by a rigid wall and by an air cavity in front of a rigid wall. For each wave propagation and surface reaction model, the surface impedance is calculated in a broad frequency range from 40 Hz to 12000 Hz at 1 Hz intervals, and for incidence angles from 0° to 90° at 1° intervals. At each frequency, the whole set of the angularly varying surface impedances is used for the extended reaction models, whereas the local reaction models use only the surface impedance at the normal incidence, assuming that the surface impedance is unchanged. The angularly varying absorption coefficients for an infinitely large panel based on the two surface reaction models are computed by equations (1) and (3). The random incidence absorption coefficients α^l_{rand} and α^e_{rand} are calculated using Paris' law [26],

$$\alpha^{e,l}_{rand}(f) = \int_0^{\pi/2} \alpha^{e,l}(f, \theta) \sin(2\theta)\, \mathrm{d}\theta. \quad (10)$$

Finally, the random incidence absorption coefficients are averaged in 1/1 octave frequency bands centered from 63 to 8000 Hz.

Unfortunately the results of this study have not been experimentally validated, because none of the existing methods, the duct method, reverberation chamber method, and free-field measurement, can measure the correct random incidence absorption coefficients. The duct method can only measure the normal incidence surface impedance, in which both reaction models yield the identical results. The reverberation chamber method can give statistical absorption coefficients in 1/1 or 1/3 octave bands based on the assumption of a perfectly diffuse field. This assumption, however, cannot be fulfilled in any reverberation chamber, and reverberation chambers are non-diffuse in different ways, resulting in large discrepancies from laboratory to laboratory [27]. Moreover, the statistical absorption coefficient is determined by an increased equivalent absorption area due to the introduction of an absorber using Sabine's formula, which basically assumes that the total absorption area is a sum of sound absorption of individual surfaces, not by the definition of the absorption coefficient, that is, a fraction of the absorbed to the incident power. Large discrepancies between the measured statistical absorption and the theoretical random incidence absorption coefficients have already been reported in the literature, e.g., see [27, 28]. Under free field conditions, the sound absorption coefficient can be measured as a function of angle of incidence. However, measurement results by the free field method can vary with the size of a specimen, the measurement location (the distance from a specimen to a sensor), the source height, the type of sensors (two microphones or a pressure-velocity probe), the type of waves considered, and the backing condition, etc., even for the simplest normal incidence cases.

As an alternative, Biot's extended reaction model is chosen to be the reference. It is not unreasonable to believe that it yields the most accurate surface impedances, since it can take into account the elastic frame resonance and interaction between the structure and fluid. To quantify differences among the calculation models, an error is defined by assuming that Biot's extended reaction model yields the true absorption coefficient,

$$e_{i,l} = \frac{1}{N_{oc}} \sum_{k=1}^{N_{oc}} \left| \frac{\alpha_{rand,i,l,k^{th}band} - \alpha_{rand,BT,ER,k^{th}band}}{\alpha_{rand,BT,ER,k^{th}band}} \right|. \quad (11)$$

Here, the subscript i means the wave propagation model (*BT* (Biot), *AC* (Allard-Champoux), *DB* (Delany-Bazley), *MK* (Miki), *BR* (Beranek)), and the subscript l

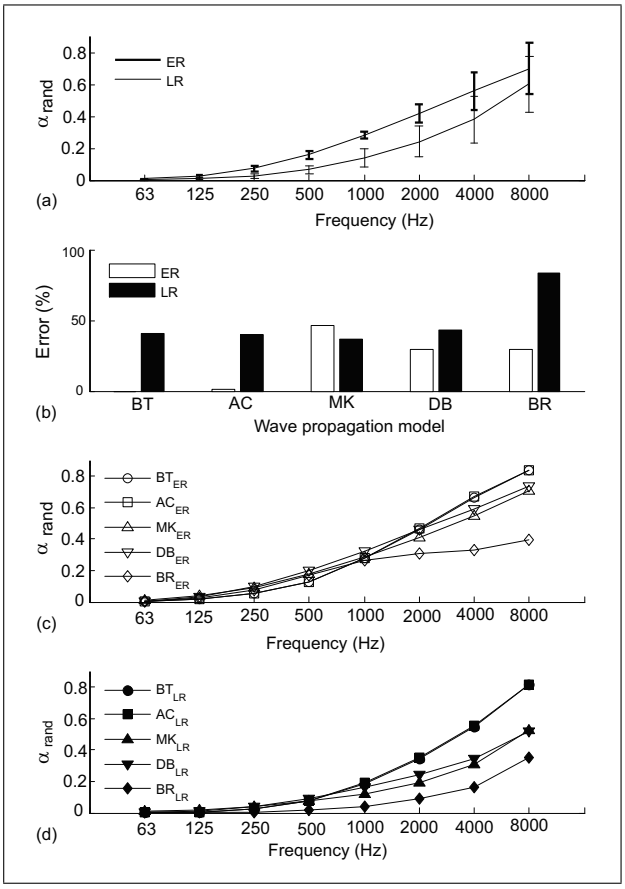

Figure 1. Random incidence absorption coefficient predicted for the rigidly backed 10 mm porous material A. (a) Mean values and 95% confidence intervals of $\alpha_{rand,ER}$ and $\alpha_{rand,LR}$, (b) error of the models, (c) $\alpha_{rand,ER}$, (d) $\alpha_{rand,LR}$.

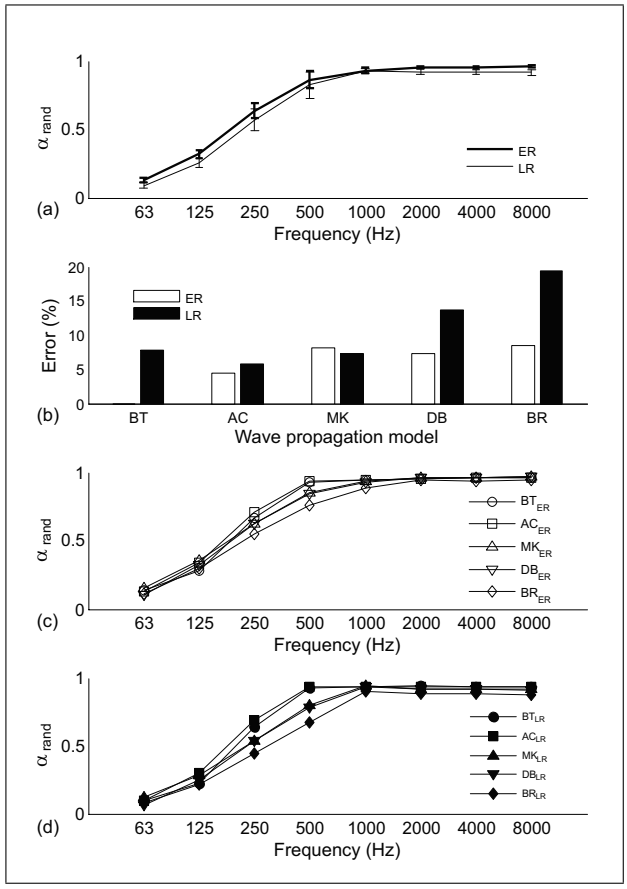

Figure 2. Random incidence absorption coefficient predicted for the rigidly backed 100 mm porous material A. (a) Mean values and 95% confidence intervals of $\alpha_{rand,ER}$ and $\alpha_{rand,LR}$, (b) error of the models, (c) $\alpha_{rand,ER}$, (d) $\alpha_{rand,LR}$.

means the surface reaction model, either extended reaction (ER) or local reaction (LR), e.g., $e_{BT,LR}$ denotes an error for Biot's local reaction model. Ten errors can be defined for an absorber under investigation, but note that $e_{BT,ER}$ is always zero. In this study, the octave band varies from 63 Hz to 8 kHz, so the number of octave bands (N_{oc}) is 8.

3.1. Porous absorbers backed by a rigid surface

For directly mounted absorbers, four porous materials with all material parameters from [12] are considered, as listed in Table II. Note that materials with a low flow resistivity is generally regarded not locally reacting [8], so a large difference between the two surface reaction models can be expected.

As the worst case, octave band random incidence absorption coefficients of a 10 mm thick porous material A (with the lowest flow resistivity of 5000 $\mathrm{Nm^{-4}s}$) predicted using the two surface reaction models are shown in Figure 1a, and the corresponding errors are displayed in Figure 1b. Figure 1a includes average values and 95% confidence intervals of the two surface reaction models. The averages, $\alpha_{rand,ER}$ and $\alpha_{rand,LR}$, in Figure 1a are the average over the five wave propagation models based on extended reaction and local reaction, respectively. Thus, the confidence intervals mean the deviations in the absorpion coefficient among the five wave propagation models. In Figure 1a, the confidence intervals do not overlap from the 125 Hz to 2 kHz octave bands, so one may conclude that the differences are statistically significant in these octave bands.

The five wave propagation models yield different results with each surface reaction model. The results of the wave propagation models are grouped into three as can be seen in Figure 1c and 1d: one includes the BT and AC model, another includes the MK and DB model, and finally the BR model alone. The AC and BT results are virtually the same in all frequency bands, but the BR model deviates significantly from the BT model, in particular at high frequencies. The deviations between the MK and DB model predictions are larger than expected, especially at around 1 kHz.

For a thicker panel of 100 mm, the error between the two reaction models is reduced to below 10%, except for the BR_LR (Beranek's local reaction model: the first acronym for the propagation model and the second for the surface reaction) and DB_LR model in Figure 2b. A similar grouping of the results is observed. However, one can use the AC_LR or MK_LR model with an error allowance of 10%. The lower frequency limit of the DB model in this case is 50 Hz, which possibly affect the absorption coefficient in

Table II. Material properties from [12].

	Frame density [kg/m^3]	Frame shear modulus [MPa]	Poisson ratio	Flow resistivity [Nm^{-4}s]	Porosity	Tortuosity	Viscous dimension [m]	Thermal dimension [m]
A	33	0.05(1+0.1j)	0.0	5000	0.98	1.10	$0.56 \cdot 10^{-4}$	$1.12 \cdot 10^{-4}$
B	16	0.09(1+0.1j)	0.0	9000	0.99	1.00	$1.92 \cdot 10^{-4}$	$3.84 \cdot 10^{-4}$
C	30	0.105+0.019j	0.4	22000	0.98	1.90	$0.56 \cdot 10^{-4}$	$1.12 \cdot 10^{-4}$
D	130	2.2(1+0.1j)	0.0	40000	0.94	1.06	$0.56 \cdot 10^{-4}$	$1.12 \cdot 10^{-4}$

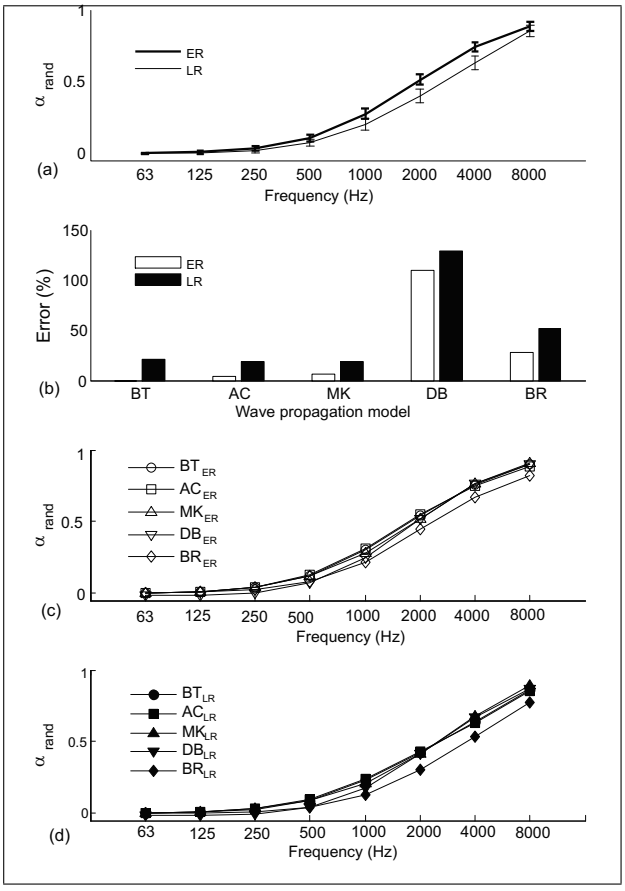

Figure 3. Random incidence absorption coefficient predicted for the rigidly backed 10 mm porous material D. (a) Mean values and 95% confidence intervals of $\alpha_{rand,ER}$ and $\alpha_{rand,LR}$, (b) error of the models, (c) $\alpha_{rand,ER}$, (d) $\alpha_{rand,LR}$.

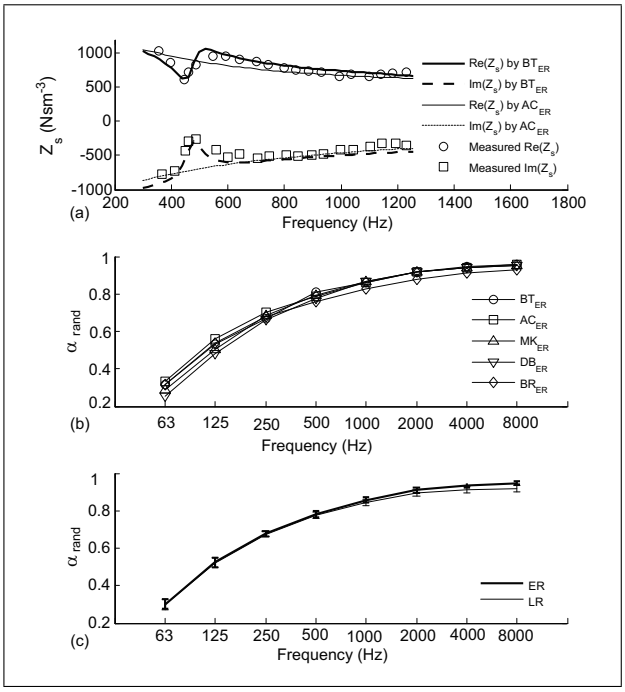

Figure 4. Normal incidence surface impedance, Z_s, and α_{rand} predicted for the rigidly backed 100 mm porous material D. (a) Z_s, measured data from [18], (b) $\alpha_{rand,ER}$, (c) mean values and 95% confidence intervals of $\alpha_{rand,ER}$ and $\alpha_{rand,LR}$.

the 63 Hz octave band. Except for the lowest frequency band, the DB result is almost the same as that of the MK model. A consistent underestimation by the BR model is observed in Figure 2c and 2d. Between the two surface reaction models, statistically significant differences at high frequencies above 2 kHz are found.

Figure 3 shows predicted random incidence absorption coefficients for a 10 mm porous material D (with the highest flow resisitivity of 40000 Nm^{-4}s). In Figure 3a, statistically significant differences between the two surface reaction models are found in the 2 kHz and 4 kHz octave bands, because the 95% confidence intervals do not overlap. The AC_ER and MK_ER model produce fairly similar results with that of the BT_ER model. In Figures 3c and 3d, the five wave propagation models do not deviate largely. However, the DB model yields negative absorption coefficients in the two lowest octave bands, since the DB model is supposed to be invalid below the lower limiting frequency of 400 Hz. Consequently the error becomes significantly larger than the others. The BR model tends to underestimate at frequencies above 500 Hz. At high frequencies, underestimation of the bulk modulus based on the isothermal process naturally leads to a decrease in the calculated random incidence absorption coefficient.

The main difference between the equivalent fluid models and the BT model is the existence of resonances of the elastic solid frame. For a 100 mm porous absorber D, a resonance peak for the frame-borne wave appears at 470 Hz in the surface impedance, which is corresponding to $\lambda/4$ in Figure 4a [12]. The effect of such a narrow resonance peak is observed in the 250 Hz and 500 Hz bands in Figure 4b, but quite negligible due to the frequency averaging (3% error in the 500Hz octave band). The five wave propagation models deviate slightly from each other at low frequencies

but, except the BR model, agree well at frequencies above 1 kHz, as can be seen in Figure 4b. The DB model still underestimates at frequencies below 500 Hz, but it gets better as the frequency increases. The difference between the two surface reaction models becomes small, but still statistically significant in the 8 kHz band in Figure 4c.

In summary, the bulk reaction random incidence absorption coefficient is likely to be higher than the local reaction absorption coefficient. Locally reacting absorbers have a constant surface impedance, and therefore it is impossible to match the surface impedance with the radiation impedance at all angles of incidence, because the radiation impedance varies with the incidence angle (for more information about the radiation impedance, see [29]), e.g., $\rho_0 c_0/\cos\theta$ for an infinite panel. So it is not unreasonable that α_{LR} is generally lower than α_{ER}. The difference between the surface reaction models is statistically significant in the high frequency bands. The largest difference between the two reaction models is found for a thin material of low flow resistivity. As the material becomes thicker and the flow resistivity becomes higher, the difference is reduced. The difference due to the resonance of the elastic frame is found to be insignificant, and thus the BT and AC model yield similar results. The BR model systematically underestimates the absorption coefficient particularly at high frequencies, and erroneous results are obtained by the DB model at frequencies lower than 0.01σ.

3.2. Porous material backed by an air gap

A surface made of the material D was chosen as the first example. The thickness of the material is 10 mm and the depth of the cavity behind the material is 450 mm, which improves the low frequency absorption performance of the element. A similar construction (a 12 mm absorber of the same material backed by a 457 mm air cavity) was used in the calculation of octave band steady-state sound pressure levels in Hodgson and Wareing's work, in which the sound pressure levels adopting Biot's extended reaction model at 63 and 125 Hz turned out to be 15 dB and 4 dB higher than those adopting Biot's local reaction model, respectively.

Figure 5 compares calculated octave band random incidence absorption coefficients for the two reaction models, showing large differences in the entire frequency range. Below 4 kHz, the local reaction models overestimate the random incidence absorption, whereas they start to underestimate above 4 kHz. The results of the two surface reaction models are statistically different except for the 4 kHz octave band. For the lowest frequency band, the DB model overestimates, which is in contrast with the rigidly backed absorber. Above the 125 Hz octave band, the DB model seems to agree well with the other models. A deviation of the BR model is noticed again at high frequencies: the BR model starts to underestimate above 2 kHz.

Figure 6 compares octave band averaged absorption coefficients as functions of incidence angle for the BT_ER and BT_LR model. At low frequencies, it is observed that the absorption coefficient of the BT_ER model decreases with increasing angle of incidence, whereas the BT_LR

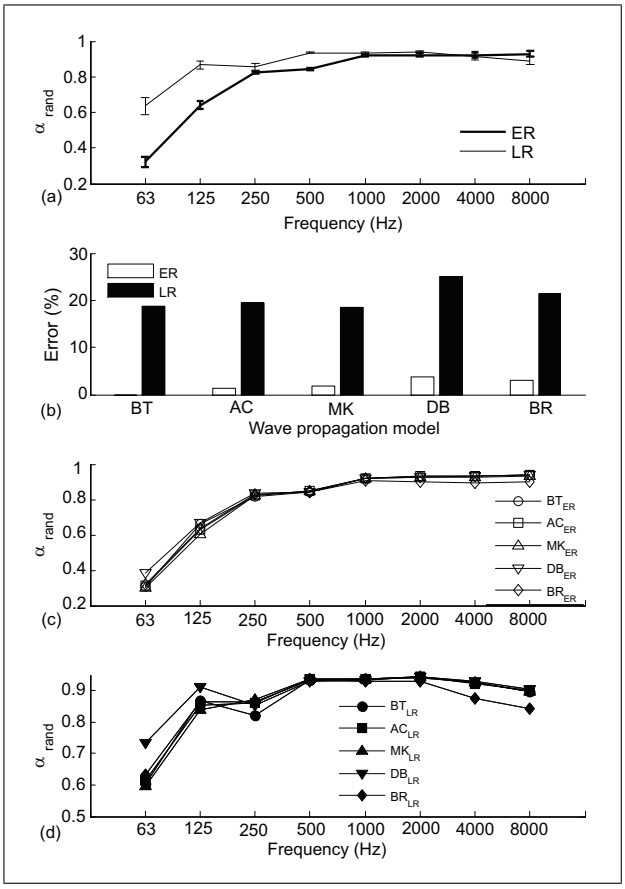

Figure 5. Random incidence absorption coefficient predicted for the 10 mm porous material D backed by a 450 mm cavity. (a) Mean values and 95% confidence intervals of $\alpha_{rand,ER}$ and $\alpha_{rand,LR}$, (b) error of the models, (c) $\alpha_{rand,ER}$, (d) $\alpha_{rand,LR}$.

model yields a curve that is nearly constant up to 60 or 70° and then steeply decreases, as can be seen in many textbooks (for example, see [30]). For infinitely large panels, the absorption coefficient at grazing incidence should vanish. Beyond the 250 Hz band, fluctuations occur in the absorption curves for extended reaction models. At higher frequencies, α_{ER} becomes higher than α_{LR}. For nearly grazing incidence, say, above 85°, the two surface reaction models agree well. Although most oblique angles of incidence yields different absorption coefficients with the two surface reaction models, good agreement is found at near-normal and near-grazing incidences. This can perhaps account for a similar result with the two surface reaction models for dissipative silencers below the cutoff frequency of a duct where only a plane wave is propagating at grazing incidence. Beyond the cutoff frequency when higher modes are excited, a predicted transmission loss calculated in a narrow frequency band starts to vary significantly, see, for example, [21], since effects of oblique incidence become dominant.

Large differences in the absorption coefficients predicted with the two surface models implicitly imply that oblique incidence surface impedances vary significantly from the normal incidence surface impedance. Therefore the surface impedance as a function of incidence angle has

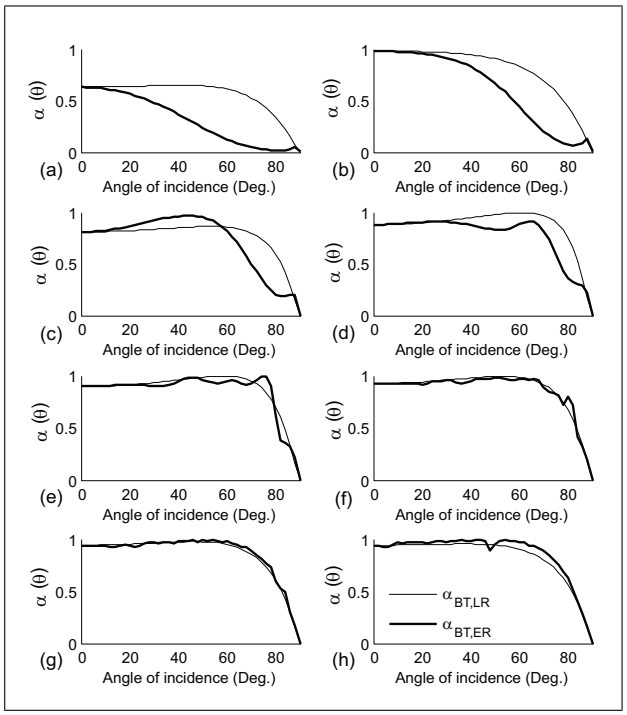

Figure 6. Octave band averaged absorption coefficient as a function of incidence angle predicted for an absorber (10 mm porous material D + 450 mm air cavity) using the Biot model. (a) 63 Hz, (b) 125 Hz, (c) 250 Hz, (d) 500 Hz, (e) 1 kHz, (f) 2 kHz, (g) 4 kHz, (h) 8 kHz.

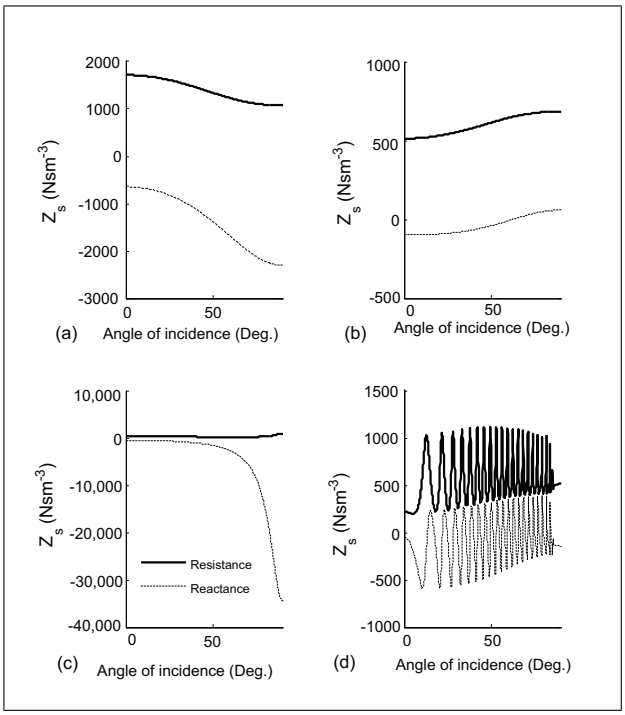

Figure 7. Surface impedances predicted as a function of incidence angle for absorbents with an air gap using the BT_ER model. (a),(b), 100 mm material backed by a 100 mm cavity; (c),(d) 10 mm material backed by a 450 mm cavity; (a),(c) 63 Hz, (b),(d) 8 kHz.

been investigated by changing the thickness ratio of the material to the cavity. Figure 7 demonstrates four cases, combining two pure tones of 63 Hz and 8 kHz and two thickness ratios of 1 (both are 100 mm thick) and 0.022 (10 mm absorber + 450 mm air cavity). Provided that the thickness of the material is comparable to the air gap depth, the surface impedance varies rather smoothly as shown in Figures 7a,b. At 63 Hz the grazingly incident surface impedance differs from the normal incidence surface impedance by a factor of 4, but the difference is reduced at 8 kHz in Figure 7b, thus can be regarded as locally reacting.

For a thickness ratio of 0.022 at 63 Hz, the grazing incidence surface impedance, particularly the reactance, changes dramatically with respect to the normal incidence case in Figure 7c. The surface impedance of the same building element changes substantially at 8 kHz in Figure 7d, but in a totally different way. The surface impedance fluctuates significantly and has many peaks that correspond to the resonances of the whole construction. However, when frequency averaging is carried out over a certain frequency range, such fluctuations will be smoothened out, as can be seen in Figure 6h. As the frequency increases, more similar random incidence absorption coefficients are obtained with the two surface reaction models, when frequency averaging is performed. Therefore relatively small differences in the predicted octave banded sound pressure levels at high frequencies between local and extended reaction in [11] can probably be attributed to the frequency averaging, and not to the fact that the surface behaves as nearly locally reacting. Thus it is of great importance to consider porous materials as non-locally reacting when the results are presented as a narrow band spectrum. However, when predicted quantities are frequency-averaged in octave bands, e.g., octave band absorption coefficients used in geometrical acoustics simulations, the results from the two reaction models would not differ significantly.

Figure 8 shows random incidence absorption coefficients calculated at every 1 Hz (without octave band averaging) based on the BT model for the two air-cavity backed absorbers from Figure 7. When the thickness of the material is comparable to the cavity depth behind, the two reaction models agree well except at low frequencies below 100 Hz in Figure 8a. When the air cavity is much thicker than the absorber, they differ significantly in Figure 8b. The local-reaction random incidence absorption fluctuate significantly, whereas the bulk-reaction absorption does not.

4. Error analysis

4.1. Errors for directly mounted absorbers

The error defined by equation (11) has been investigated by changing the thickness from 20 mm to 400 mm and the flow resistivity from 5000 to 40000 $\mathrm{Nm^{-4}s}$. Averaged errors for the two reaction models are displayed in Figure 9 for the four different materials; e_{ER} is the average error over the extended reaction models except the BT_ER

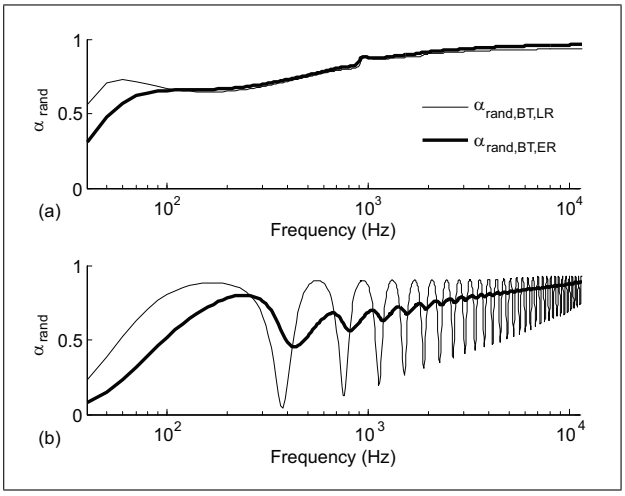

Figure 8. Random incidence absorption coefficient predicted for absorbers with an air gap as a function of frequency employing the *BT* model. (a), 100 mm material backed by a 100 mm cavity; (b) 10 mm material backed by a 450 mm cavity.

model, since $e_{BT,ER}$ is 0, and e_{LR} is defined in the same way. Generally, e_{LR} is higher than e_{ER}, and they both decrease with increasing thickness. To achieve an error allowance of 10% with the extended reaction modeling, the absorber thickness should be larger than 35 mm for material D, 50 mm for material C, 55 mm for material A, and 60 mm for material B. It seems that e_{ER} does not significantly depend on the flow resistivity.

For the local reaction models, the errors depend strongly on the thickness and the flow resistivity. Because materials with high flow resistivity are more likely to react locally, the error for the local reaction becomes lower, as the flow resistivity increases. The thicker the material, the lower the error. Required thicknesses to reduce e_{ER} to less than 10% vary from 40 to 120 mm: 40 mm for material D, 60 mm for material C, 100 mm for material B, and 120 mm for material A. Approximately, a 25 mm thinner material is required for doubling the flow resistivity. However, note that this is a guideline for calculating octave band random incidence absorption coefficients with the assumption of local reaction, which does not imply that a porous absorber made of material A thicker than 120 mm is locally reacting. The error for material B behaves slightly different with the other materials. The error becomes a little higher than 10% for a certain range of the thickness from 250 to 350 mm, where $\alpha_{rand,BT,ER}$ differs from the others due to the frame resonance at $\lambda/4$. For material D which has the highest flow resistivity, the error is the lowest for a thin material.

Figure 9c compares different extended reaction models for material A. The $e_{AC,ER}$ is nearly independent of the absorber thickness for all the samples, while the errors of the other models are dependent on the material thickness. Thus the AC_ER model is the best alternative, if the BT_ER cannot be employed. For thin absorbers, $e_{MK,ER}$ is the largest, whereas $e_{BR,ER}$ is the largest for thicker absorbers. The MK_ER model produces the largest error for a thin material, but the error is reduced as the thickness increases.

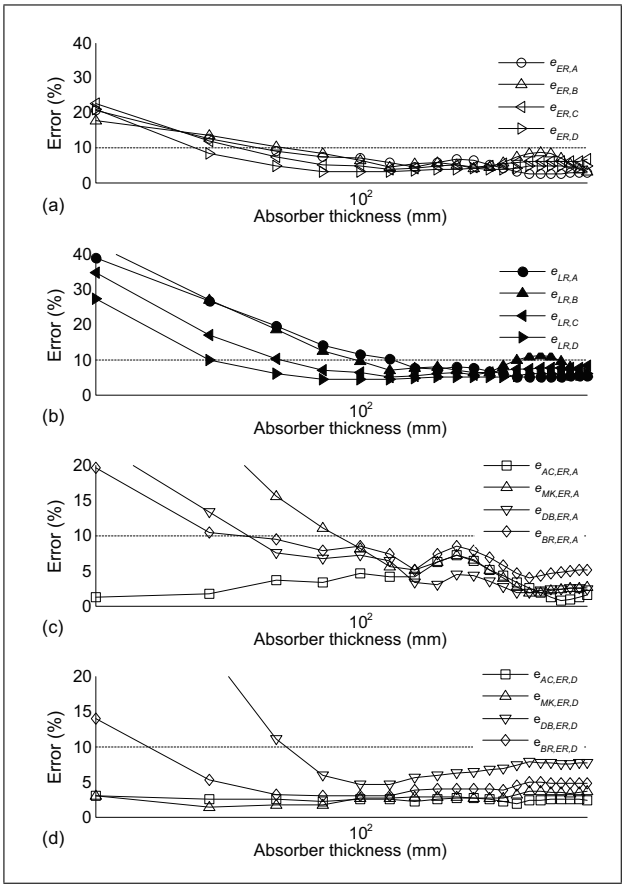

Figure 9. Predicted errors for rigidly backed absorbents as a function of the thickness. (a) e_{ER} for the four materials, (b) e_{LR} for the four materials, (c) e_{ER} for material A, (d) e_{LR} for material D.

Figure 9d compares different extended reaction models for material D. For materials with a high flow resistivity, the lower limit frequency of the DB model is likely to be higher than 63 Hz, and thus $e_{DB,ER}$ becomes large. However, its modified version, the MK_ER model, agrees well with the BT_ER model regardless of the thickness, as the AC_ER model does. Thus the AC_ER model and MK_ER model are the best alternative to the BT_ER model for high flow resistivity cases.

4.2. Errors for absorbers with a backing air gap

The errors of the two reaction models for the four materials are shown in Figures 10a and 10b for different absorber thicknesses from 20 mm to 400 mm in steps of 20 mm for a fixed cavity depth of 300 mm. The abscissa is the thickness ratio of the absorber to the air gap. The accuracy of the extended reaction models is not strongly influenced by the thickness ratio if the ratio is above 0.1. All the extended reaction models produce reliable results in terms of the 10% error criterion. However, the precision of the local reaction models is affected by the thickness ratio. With a 10% error criterion for the local reaction models, the thickness ratio of material A should be 0.37, and 0.32 for material B, 0.2 for material C, 0.1 for material D. As the flow resistivity

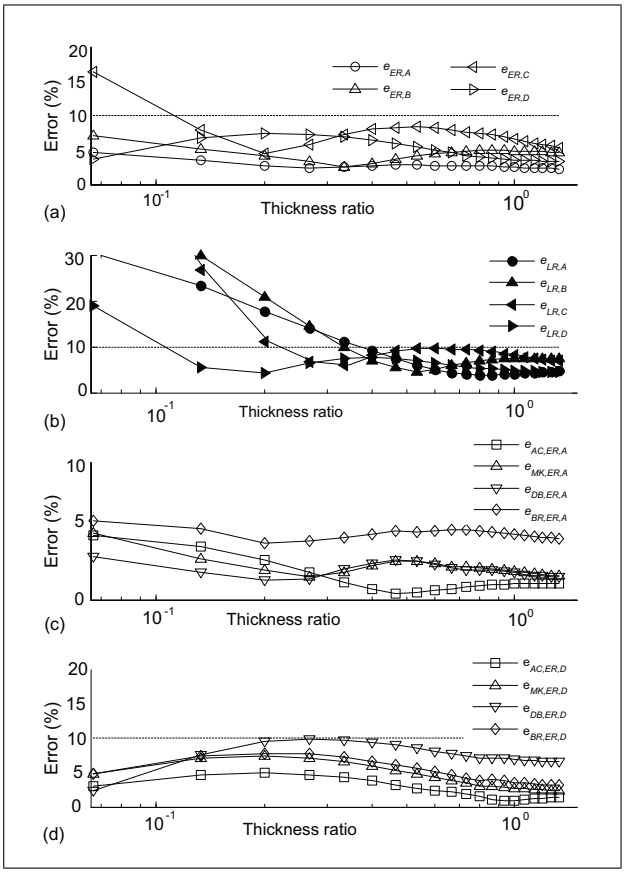

Figure 10. Predicted errors for absorbents with an air gap as a function of the thickness ratio. (a) e_{ER} for the four materials, (b) e_{LR} for the four materials, (c) e_{ER} for material A, (d) e_{ER} for material D.

is increased, the required thickness ratio decreases. Again, approximately a decrease in the required thickness ratio by 0.1 for doubling the flow resistivity is found for the local reaction models.

Figure 10c compares different extended reaction models for material A. The errors of the extended reaction models are nearly constant regardless of the model. The AC_ER model yields the accurate results on average, whereas the BR results deviate for high thickness ratios, but is still within an error bound of 5%.

Figure 10d compares different extended reaction models for material D. Any extended reaction models produce errors of less than 10%. Among the extended reaction models, the AC_ER model is the best, and the MK_ER model also yields quite reliable results.

Table III depicts differences between $\alpha_{rand,ER}$ and $\alpha_{rand,LR}$ for a 10 mm material D backed by various air cavities from 50 mm to 350 mm, indicating that the frequency at which the maximum difference occurs decreases with increasing cavity depth, e.g., a maximum difference occurs at a lower frequency with a larger air cavity. Therefore it can be concluded that room surfaces should not be modeled as local reacting for porous materials backed by a large cavity, in particular when the thickness ratio is lower than 0.4.

Table III. Difference between predicted extended-reaction and local-reaction absorption coefficients obtained by changing the air cavity depth for a 10 mm absorber D. The maximum differences are highlighted in bold. Cavity depths from 50 mm to 350 mm. f_c: Center frequency (Hz).

f_c	50 mm	150 mm	250 mm	350 mm
63	0.03	0.14	0.24	**0.29**
125	0.08	0.26	**0.31**	0.28
250	0.17	**0.27**	0.19	0.10
500	**0.22**	0.12	0.06	0.12
1k	0.13	0.09	0.04	0.03
2k	0.06	0.03	0.01	0.01
4k	0.01	0.00	0.01	0.01
8k	0.03	0.02	0.04	0.01

4.3. Comparison with other experimental results

Bliss and Burke examined three oblique angles of 9°, 45°, and 81°, and concluded that bulk reaction increases the absorption coefficient significantly [16]. The bulk reaction absorption coefficient calculated for a 25.4 mm fiberglass board is 39% higher than the local reaction absorption coefficient from 200 to 1200 Hz. This conclusion concurs with the directly mounted thin material A in Figure 1, but unfortunately Bliss and Bruke did not specify the flow resistivity of the material, Owens-Corning PF-705. Klein and Cops showed that the surface impedance of a polyurethane foam layer changes with angle of incidence at 10° intervals, in which the surface impedance varies significantly above 60° [15]. Sides and Mulholland measured the surface impedance of low density rockwool, and found extended reaction at 500 Hz, whereas they concluded that the material is locally reacting at 2000 Hz [17]. Shaw compared angularly varying absorption coefficients predicted from normal incidence surface impedance and from measured angularly varying surface impedance of a 12.7 mm hairfelt sample at 1250 Hz [18]. The bulk reaction absorption coefficient was found to be higher than the local reaction absorption, which also concurs with the result of the present study. The previous studies concluded that rigidly backed porous materials cannot be treated as locally reacting, if they are thin. Unfortunately, the author cannot find experimental results of an absorber backed by an air gap, which show discrepancies between the bulk reaction and local reaction.

5. Conclusions

Random incidence absorption coefficients based on extended and local reaction have been compared for five wave propagation models. For rigidly backed porous materials, the assumption of local reaction always underestimates the random incidence absorption coefficient. Large differences for low flow resistance cases have been found, in particular at low frequencies. The two surface reaction models agree better for higher resistivity cases and thicker absorbers. It is noticed that the DB model tends to underestimate at lower frequencies, whereas the BR

model tends to underestimate above a few thousand hertz. To achieve an error of less than 10%, a material with a flow resistivity of 5000 $\mathrm{Nm^{-4}s}$ should be thicker than 120 mm, whereas a dense material with a flow resistivity of 44000 $\mathrm{Nm^{-4}s}$ needs to be only 40 mm thick. Unlike the local reaction models, the accuracy of the extended reaction models does not depend strongly on the flow resistivity. The AC_ER model shows a nearly similar performance with the BT_ER model regardless of the thickness and the flow resistivity.

For absorbers with an air gap, a large difference between the two reaction models was found, because the surface impedance at oblique incidence is noticeably different from the normal incidence surface impedance. For low thickness ratios, the local reaction model overestimates significantly at low frequencies, whereas it underestimates slightly at high frequencies. Relatively small differences at high frequencies for low thickness ratios are ascribed to the frequency averaging in octave bands. As the thickness ratio is increased, such discrepancies between the two surface reaction models are reduced. If the thickness ratio becomes larger than 0.4, two surface reaction models yield similar random incidence absorption coefficients. Any of the examined extended reaction model yields reliable results for thickness ratios above 0.1.

Among the models studied, the AC_ER model had the best agreement with the BT_ER model, making it the most accurate among the other models. However, for absorbers backed by an air cavity and directly mounted absorbers with high flow resistivity, the MK_ER models can also be used. The DB model and BR model have clear limitations at low frequencies and high frequencies, respectively, and thus it is advised not to use these models in the entire audible frequency range.

References

[1] M. E. Delany, E. N. Bazley: Acoustical properties of fibrous absorbent materials. Appl. Acoust. **3** (1970) 105–116.

[2] Y. Miki: Acoustical properties of porous materials - modifications of Delany-Bazley models. J. Acoust. Soc. Jp. **11** (1990) 19–28.

[3] L. L. Beranek: Acoustic impedance of porous materials. J. Acoust. Soc. Am. **13** (1962) 248–260.

[4] J.-F. Allard, Y. Champoux: New empirical equations for sound propagation in rigid frame fibrous materials. J. Acoust. Soc. Am. **91** (1992) 3346–3353.

[5] M. A. Biot: Theory of propagation of elastic waves in a fluid-saturated porous solid. I. Low frequency range, II. Higher frequency range. J. Acoust. Soc. Am. **28** (1956) 168–191.

[6] S. K. Kakoty, V. K. Roy: Bulk reaction modeling of sound propagation through circular dissipative ducts backed by an air gap. J. Vib. Acoust. **128** (2006) 699–704.

[7] U. J. Kurze, I. L. Ver: Sound attenuation in ducts lined with non-isotropic material. J. Sound Vib. **24** (1972) 177–187.

[8] K. M. Li, T. Waters-Fuller, K. Attenborough: Sound propagation from a point source over extended-reaction ground. J. Acoust. Soc. Am. **104** (1998) 679–685.

[9] H. Utsuno, T. W. Wu, A. Seybert, T. Tanaka: Prediction of sound fields in cavities with sound absorbing materials. AIAA J. **28** (1990) 1870–1876.

[10] L. P. Franzoni, C. M. Elliott: An angle-by-angle approach to predicting broadband high-frequency sound fields in rectangular enclosures with experimental comparison. J. Acoust. Soc. Am. **114** (2003) 1968–1979.

[11] M. Hodgson, A. Wareing: Comparisons of predicted steady-state levels in rooms with extended- and local-reaction bounding surfaces. J. Sound Vib. **309** (2008) 167–177.

[12] J.-F. Allard, N. Atalla: Propagation of sound in porous media: Modelling sound absorbing materials. 2nd edition. John Wiley and Sons, London, 2009.

[13] T. Cox, P. D'Antonio: Acoustic absorbers and diffusers. Spon Press, London, 2004. 23.

[14] K. Attenborough: Acoustical characteristics of porous materials. Phys. Rep. **82** (1982) 179–227.

[15] C. Klein, A. Cops: Angle dependence of impedance of a porous layer. Acustica **44** (1980) 258–264.

[16] D. B. Bliss, S. E. Burke: Experimental investigation of the bulk reaction boundary condition. J. Acoust. Soc. Am. **71** (1982) 546–551.

[17] D. J. Sides, K. J. Mulholland: The variation of normal layer impedance with angle of incidence. J. Sound Vib. **14** (1971) 139–142.

[18] E. A. G. Shaw: The acoustic wave guide. II. Some specific normal acoustic impedance measurements of typical porous surfaces with respect o normally and obliquely incident waves. J. Acoust. Soc. Am. **25** (1953) 231–235.

[19] F. P. Mechel: Ausweitung der Absorberformel von Delany und Bazley zu tiefen Frequenzen (Extension to low frequencies of the formulae of delany and bazley for absorbing materials). Acustica **35** (1976) 210–213.

[20] T. Komatsu: Improvement of the Delaney-Bazley and Miki models for fibrous sound-absorbing materials. Acoust. Sci. & Tech. **29** (2008) 121–129.

[21] H.-J. Kim, J.-G. Ih: Rayleigh-Ritz approach for predicting the acoustic performance of lined rectangular plenum chambers. J. Acoust. Soc. Am. **120** (2006) 1859–1870.

[22] A. Cummings: High frequency ray acoustics models for duct silencers. J. Sound Vib. **221** (1999) 681–708.

[23] L. J. Sivian: Sound propagation in ducts lined with absorbing materials. J. Acoust. Soc. Am. **9** (1938) 135–140.

[24] Y. Champoux, J.-F. Allard: Dynamic tortuosity and bulk modulus in air-saturated porous media. J. Appl. Phys. **70** (1991) 1975–1979.

[25] D. L. Johnson, J. Koplik, R. Dashen: Theory of dynamic permeability and tortuosity in fluid saturated porous media. J. Fluid Mech. **176** (1987) 379–402.

[26] E. T. Paris: On the coefficient of sound-absorption measured by the reverberation method. Phil. Mag. **5** (1928) 489–497.

[27] C. W. Kosten: International comparison measurement in the reverberation room. Acustica **10** (1960) 400–411.

[28] C.-H. Jeong: A correction of random incidence absorption coefficients for the angular distribution of acoustic energy under measurement conditions. J. Acoust. Soc. Am. **125** (2009) 2064–2071.

[29] J. H. Rindel: Modeling the angle-dependent pressure reflection factor. Appl. Acoust. **38** (1993) 223–234.

[30] H. Kuttruff: Room acoustics. 4th edition. Spon Press, London, 2000.